Shape Control of the Tension Truss Antenna

Jin Mitsugi* and Tetsuo Yasaka†
NTT Radio Communication Systems Laboratories, Yokosuka, Japan
and
Koryo Miura‡
Institute of Space and Astronautical Science, Sagamihara, Japan

The tension truss antenna is a deployable mesh surface antenna featuring a cable network, called a tension truss, that gives a parabolic shape to the reflective mesh. Cables in the tension truss are rigid enough to prevent their elongation due to the tension, and the number of nodes and cables satisfies the statically determinant condition. In this paper, surface sensitivity to magnitude and direction errors of the applied force, which gives the tensile force to the tension truss, is evaluated by Monte Carlo simulation. Results show that the surface deformation of a tension truss antenna is smaller than that of an antenna whose cable network is made of flexible cables. A surface control algorithm is derived using the perturbation method, and numerical simulations and experimental verifications of the algorithm are carried out. Results show that the surface shape of a tension truss antenna can be controlled by changing cable lengths, and local surface deformations can be improved without affecting the shape of the other parts of the surface. It is concluded that the tension truss antenna is a promising candidate for a large space antenna.

Introduction

THE need for large deployable antennas has been presented in various scientific fields such as satellite communication, space observation, and Earth resource sensing. The antennas are required to be lightweight and deployable to meet the restrictions of the launcher capability. They also must have sufficient surface accuracy and aperture area to accomplish their missions.

Several concepts for large deployable antennas have been presented, such as foldable rigid petals, mesh with deployable ribs, a rigid surface with deployable truss, and an inflatable rigidizing antenna. These antennas can be classified into two groups: rigid-surface antennas and mesh surface antennas. Rigid-surface antennas can achieve high surface accuracy, but there are difficulties in their packaging method and efficiency. On the other hand, mesh surface antennas have less accurate reflector surface than the rigid surface type, but they can be packaged easily and compactly. Since the surface error should be smaller than about 0.02λ[1] (λ denotes wavelength) to obtain appropriate antenna gain, high-frequency antennas usually need rigid-surface reflectors, and relatively low-frequency antennas normally employ mesh surface reflectors. Large mesh reflectors are expected to be used for a number of uhf to S-band missions.

In most mesh surface antenna concepts, a reflective mesh is attached to a parabola-shaped cable network. Therefore, the shape of the reflective surface is determined by the shape of the cable network. However, it seems that not enough attention has been paid to the research on cable networks. The shape of a conventional mesh antenna is determined by the equilibrium of forces in the cable network. Thus, the shape control algorithm of this kind of antenna must include the influence function that describes the effect of cable lengths or force variations on the surface shape. The influence function can be derived from the relationship between the shape and applied forces, and generally finite-element models are used. Reference 2 mentions shape control of a hoop column antenna using linearized sensitivity analysis.

The purpose of this study is to evaluate the concept of a tension truss antenna developed to simplify the shape control procedure. The procedure is simplified by using rigid cables and a statically determinant condition in the cable network. By doing this, the effect of strains and nonlinearity in the cable network is expected to be reduced, thereby reducing the complexity of deriving the influence function.

Tension Truss Antenna Description

The tension truss antenna (TTA) is composed of a reflective mesh, cable network called a tension truss, a supporting cable network that provides tension to the cables in the tension truss, and a deployable structure that supports cable networks. The reflective mesh attached to the tension truss forms a reflective surface of the antenna. The unique feature of the TTA is its tension truss, which can be considered a statically determinant truss structure composed of cables.

A statically determinant truss structure satisfies Maxwell's criteria $L = DOF$, where L denotes the number of truss members, and DOF denotes the unconstrained degree of freedom in the system. Node positions of an unloaded statically determinant truss structure are determined only by the lengths of truss members and their arrangement. The shape can be modified by changing the lengths of truss members; changing the lengths of truss members causes no internal forces in the structure.

Cables in a tension truss can behave like members of an unloaded statically determinant truss structure if they are subjected to the following conditions:

1) The cables are subjected to tensile force, since they have no rigidity to compressive forces.

2) The cables are inextensible or the strains are small enough to be neglected, in order to prevent the elongation of cables due to tension.

If a cable network is constructed to keep these conditions and the statically determinant condition, it is a tension truss. Since a tension truss can be considered a statically determinant

Received May 23, 1988; revision received Feb. 15, 1989.

*Research Engineer, Communication Satellite Technology Laboratory.

†Executive Research Engineer, Communication Satellite Technology Laboratory. Member AIAA.

‡Professor. Member AIAA.

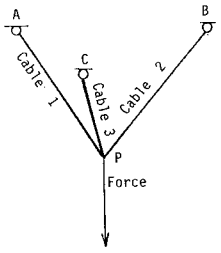

Fig. 1 Tension truss concept.

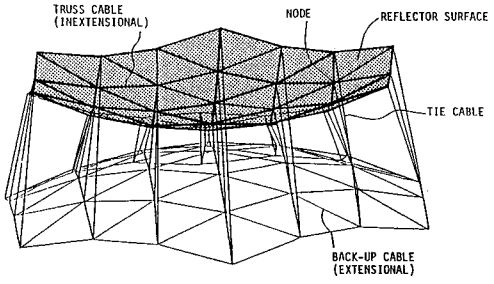

Fig. 2 Tension truss antenna.

truss structure, node positions in a tension truss are determined by the lengths and the arrangement of its cables, and modification causes no large change of internal forces in the network. Large change of internal forces should be avoided, since they may slacken cables, and slackening of cables causes large antenna surface deformation.

The concept of the tension truss is illustrated in Fig. 1. Nodes A, B, and C are fixed points provided by the supporting structure. Cables 1, 2, and 3 are inextensible cables. A force is applied to give tension to the cables, and the number of cables (3) and the unconstrained degree of freedom (translations of node P = 3) satisfy the statically determinant condition. Therefore, the cable network composed of cables 1, 2, and 3 is a tension truss. The position of node P is determined not by the magnitude and direction of the applied force but by the lengths of the three cables. The applied force exists only to give tensile forces to the cables. This is the basic concept of the tension truss and its shape control. A TTA can be constructed by extending this basic concept, as shown in Fig. 2. In this figure, the reflector surface is composed of a tension truss and a reflective mesh attached to the tension truss. Tie cables and backup cables provide tensile forces to the tension truss. They should be extensible cables to provide the tensile forces easily. Since node positions can be determined by lengths of tension truss cables, surface deformations can be corrected by changing the lengths of the tension truss without considering any equilibrium of forces in the cable networks.

In order to verify the concept of the TTA, a 3-m-diam model was fabricated (Fig. 3). The cables are made of 0.6-mm-diam Kevlar wires, and each cable has a turnbuckle, which modifies the cable length, at midcord. Each node has a fitting to connect it to the cables. In this model, the supporting structures are six radially extendable "hingeless masts."[3] These masts are stowed in the central hub and deployed synchronously by the electric controller. At full extension, they provide tensile forces to the tension truss through the tie cables and backup cables. To prevent deformation of the six radial masts due to gravity, the seventh mast is placed along the vertical symmetric axis. Six radial masts are hoisted by the cables connected to the seventh central mast, and hoisting tensions are adjusted by counterweights to cancel the gravitational bending moment in the six radial masts.

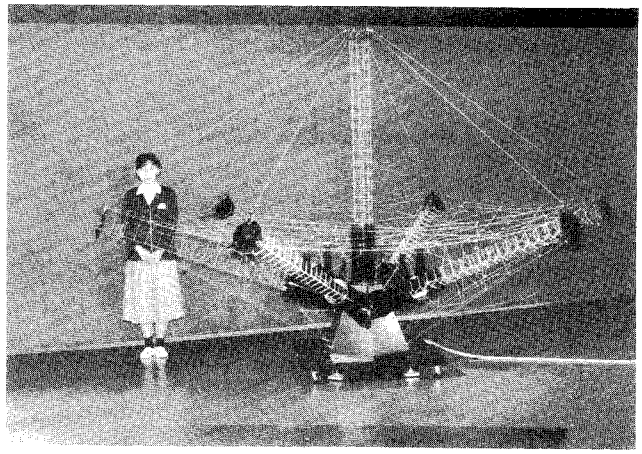

Fig. 3 Concept model.

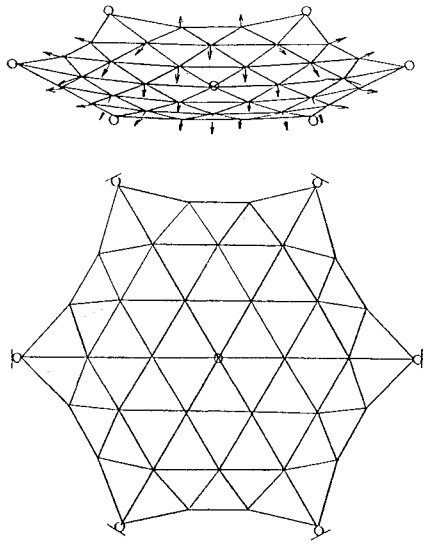

Fig. 4 Calculation model and applied forces.

Surface Sensitivity Analysis

Although cables in a tension truss are assumed to be rigid, there are some strains due to tensile forces. This analysis numerically clarifies the effects of such small strains on the surface shape. Surface sensitivity to such applied force error is estimated in terms of the expected rms surface error using the Monte Carlo simulation technique. Calculations are carried out on the antenna surface model shown in Fig. 4, which satisfies the statically determinant condition. Two focal length-to-diameter ratios ($F/D = 1.5$ and 3.5) and two cable elongation rigidities are considered. Elongation rigidities are expressed in terms of the initial strain (initial tension/cable rigidity). Since the initial tension of all cables is set to be the same, a smaller initial strain (2×10^{-5}) means a cable network composed of rigid cables, implying a tension truss. In the same way, a larger initial strain (2×10^{-3}) implies a flexible cable network. A tension truss with an initial strain on this order (10^{-5}) can be made of existing materials, for example, about 1-mm-diam Kevlar wire with 0.2-kgf tension in the cables.

Calculations were carried out using the Cable Structure Analysis Code (CASA), which is an originally developed program written in FORTRAN (Fig. 5). CASA requires initial cable lengths, applied forces, and the cable arrangement as input data and calculates the resultant node positions and strains in the cables.

The potential energy of the cable network is the strain energy due to tensile forces in the cables and can be expressed as

$$P=\Sigma_c[(|X_{i2}-X_{i2}|-l_i)/l_i]^2(EA)_i l_{i/2} \quad (1)$$

where i denotes the node identification number, X_{i1}, and X_{i2} denote the position vectors of the terminal nodes of the ith cable, l_i denotes the length of ith cable, $(EA)_i$ is the elongation rigidity (Young's modulus times cross-sectional area) of the ith cable, and Σ_c is the summation of all cables.

Variation of the potential energy is

$$\delta P=\Sigma_c(EA)_i(|X_{i1}-X_{i2}|-l_i)/(l_i|X_{i1}-X_{i2}|)(X_{i1}-\mathbf{X}_{i2}) \times(\delta X_{i1}-_{i2}). \quad (2)$$

External virtual work is given by the applied forces at nodes

$$\delta F=\Sigma_n fj(X_{fj}-X_j)/|X_{fj}-X_j|\delta X_j \quad (3)$$

where X_{fj} is the position vector of the fix point to which the force vector imposed on j-th node X_j orients, and Σ_n means the summation of all nodes. The scalar value of the applied force is fj.

Equations for determination of the node positions in the cable network are derived using Hamilton's principle:

$$\delta P-\delta F=0 \quad (4)$$

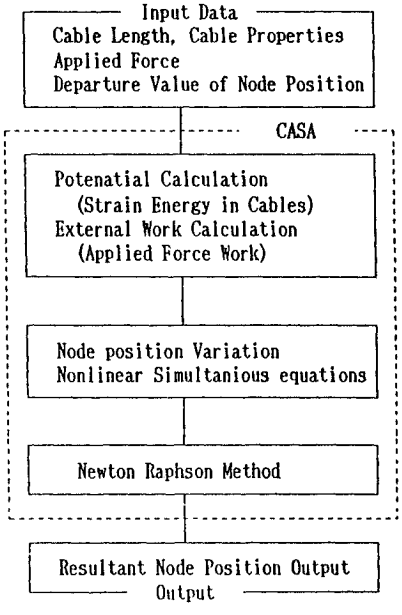

Fig. 5 CASA flowchart.

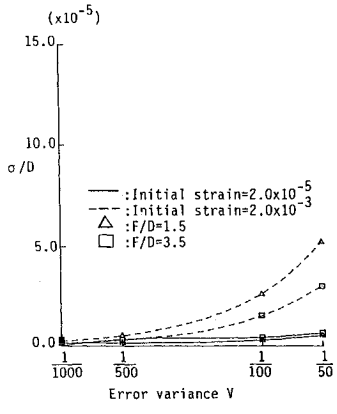

Fig. 6 Surface error due to applied force magnitude error.

CASA calculates the resultant node positions using the Newton-Raphson method to satisfy these equations. In the calculation, the nonlinear Young's modulus of a cable, which is equal to zero in the compression, is taken into consideration.

In the sensitivity analysis, the magnitude and the direction of the applied forces are determined once to give all cables equal tension (equal strain) and arrange the nodes on a design parabola. Then, magnitude and direction values are multiplied by an error factor obtained from a random number generator. CASA calculates the resultant node positions using this altered data, and the expected surface rms error is determined by using the Monte Carlo simulation. Even if all of the nodes are on the design parabola, the expected rms error is on the order of 10^{-6}. This residual error is caused by the reduced significant figures of input data.

Magnitude Variation

Sensitivities of a tension truss and a flexible cable network to the applied force magnitude errors are calculated as shown in Fig. 6. In the figure, V denotes the standard variance of the applied force magnitude error. For example, $V=1/50$ means that the magnitude of applied forces is multiplied by error factors, whose mean value is equal to 1.0 and the standard variance is equal to 1/50. The σ/D denotes the surface rms error expectation nondimensionalized by the antenna aperture. This expectation is obtained using 50 trials of Monte Carlo simulation. Results show that the surface error increases corresponding to increases in applied force error variance. This comes from the strain variation of cables due to applied force error. A TTA has a surface that is stable with applied force variation because the elongation of TTA cables due to the applied force error is smaller than that of cables in a flexible cable network. Large F/D antennas have a surface that is more stable with regard to the applied force error than small F/D antennas because the initial cable length in large F/D antennas is shorter in small F/D antennas.

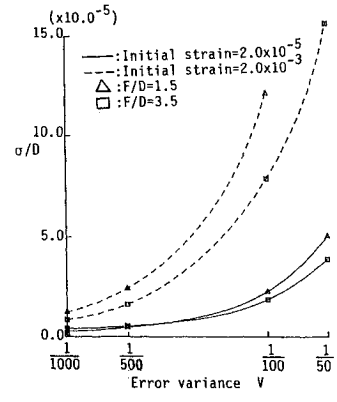

Fig. 7 Surface error due to applied force direction error.

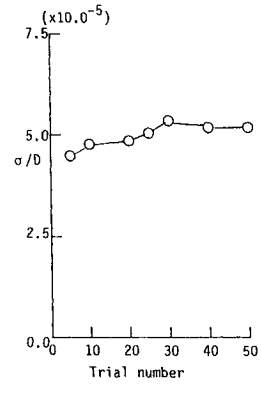

Fig. 8 Effect of trial number on Monte Carlo simulation.

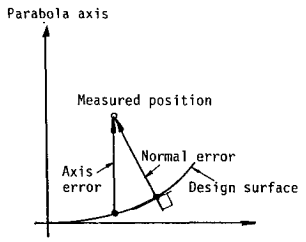

Fig. 9 Error vector definition.

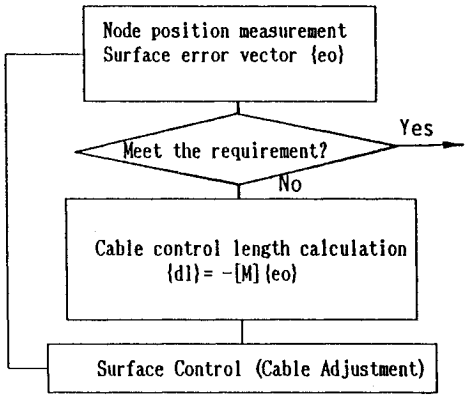

Fig. 10 Shape control algorithm.

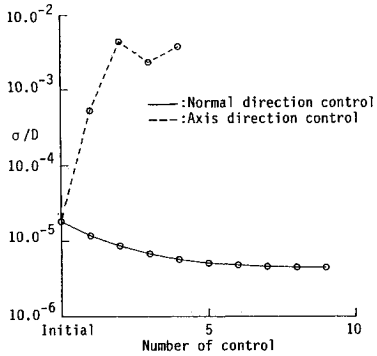

Fig. 11 Shape control sequence.

Direction Variation

As mentioned in the previous section, the applied force vectors to give all cables equal tension and make all nodes be on the design parabola. Each force is assumed to be applied through a 3/40D long tie cable, which is attached to the respective external point. The applied force direction error is generated by multiplying the error factor, whose mean value is 1.0 and standard variance is V to the X, Y, Z coordinates of the fixed point. The results are shown in Fig. 7. As in the case of magnitude variation, the TTA is stable in relation to the variation in the applied force direction. This stability is shown by the fact that elongations and shortenings of the rigid cables due to the applied force variation are small. Large F/D antennas show stability in relation to direction error.

The results of the Monte Carlo simulation for several trial numbers is shown in Fig. 8. Although the number of trial calculations in the preceding discussion is 50, 20 trials are considered to provide a good approximation.

Shape Control of Tension Truss Antenna

A TTA modifies its shape by changing the lengths of cables in the tension truss. Its modifications can be performed like those of a statically determinant truss structure. However, iterations of shape control are necessary, since a real tension truss has strains in cables, and cable length changes result in the strain changes. In this section, a linearized shape control algorithm is derived by using the perturbation method, and numerical simulations, which consider the cable elasticity, show the propriety of the shape control method. Experimental verification of the shape control is also carried out.

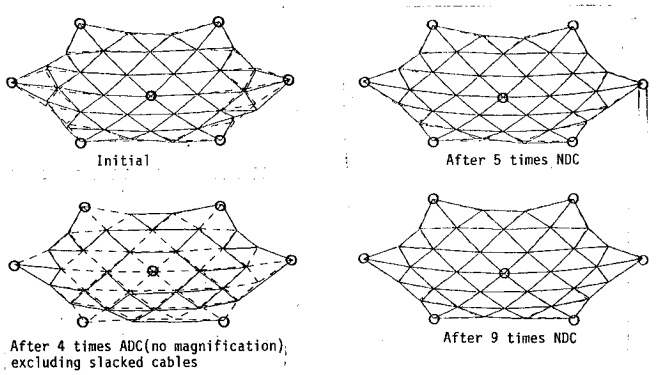

Fig. 12a Shape control sequence; initial strain = 2.0×10^{-2}.

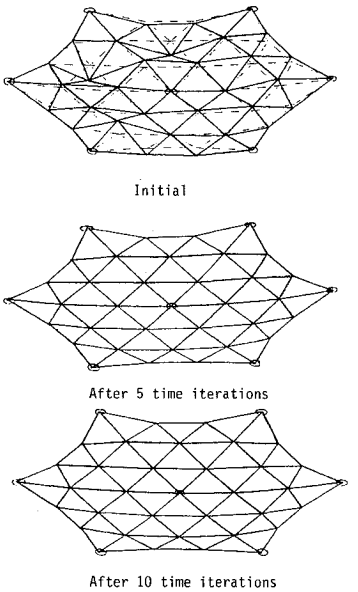

Fig. 12b Shape control sequence; initial strain = 2.0×10^{-4}.

Surface Control Algorithm

Relationships between the cable lengths and the node positions are expressed by the following simultaneous equations:

$$l_1 = (X_{11} - X_{12})^2 + (Y_{11} - Y_{12})^2 + (Z_{11} - Z_{12})^2 \quad (5a)$$

$$l_N = (X_{N1} - X_{N2})^2 + (Y_{N1} - Y_{N2})^2 + (Z_{N1} - Z_{N2})^2 \quad (5b)$$

where N is the number of cables, l_i denotes the length of the ith cable, and X_{ij}, Y_{ij}, Z_{ij} $(j = 1,2)$ are X, Y, Z coordinates of the nodes on both ends of the ith cable.

The perturbation equations are given as

$$l_1 dl_1 = (X_{11} - X_{12})(dX_{11} - dX_{12}) + (Y_{11} - Y_{12})(dY_{11} - dY_{12}) + (Z_{11} - Z_{12})(dZ_{11} - dZ_{12}) \quad (6a)$$

$$l_N dl_N = (X_{N1} - X_{N2})(dX_{N1} - dX_{N2}) + (Y_{N1} - Y_{N2})(dY_{N1} - dY_{N2}) + (Z_{N1} - Z_{N2})(dZ_{N1} - dZ_{N2}) \quad (6b)$$

After eliminating the perturbed terms of the fixed nodes, these equations can be expressed simply using $\{dl\}$, $\{dx\}$, and $[M]$:

$$\{dl\} = [M]\{dX\} \tag{7}$$

where $\{dl\} = \{dl_1 \ldots dl_N\}T$, $[M] = [M_{ij}]$, $\{dX\} = \{dX_1\ dY_1\ dZ_1 \ldots dX_m\ dY_m\ dZ_m\}^T$, and m denotes the number of unconstrained nodes ($3m = N$).

Observation of the matrix $[M]$ clarifies that lengths of the cables, which are connected to the controlled node, should be changed to translate the node, as long as the rigid-cable assumption is employed. This means that the surface shape can be controlled by changing lengths of cables only in the vicinity of the control area.

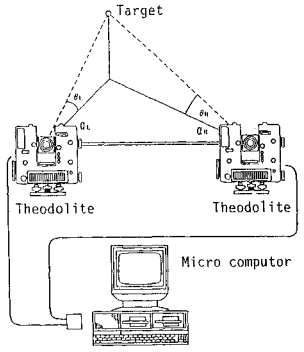

Fig. 13 Position measurement system.

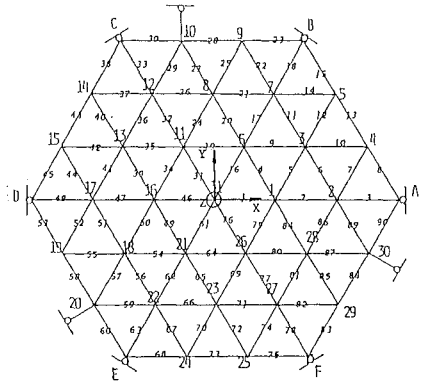

Fig. 14 Node and cable identification and coordinate system.

Table 1 Control cable lengths

	$dZr = -1$ mm	$dZr = -2$ mm	$dZr = -3$ mm
dl_5	−0.1791	−0.3582	−0.5373
	(−0.1771)	(−0.3504)	(−0.5200)
dl_6	0.0992	0.1985	0.2978
	(0.1011)	(0.2064)	(0.3155)
dl_9	−0.1811	−0.3623	−0.5434
	(−0.1792)	(−0.3546)	(−0.5261)
dl_{10}	0.3524	0.7048	1.0572
	(0.3541)	(0.7113)	(1.0719)
dl_{11}	0.1043	0.2086	0.3130
	(0.1063)	(0.2164)	(0.3307)
dl_{12}	0.3447	0.6894	1.0341
	(0.3463)	(0.6961)	(1.0490)

The effect of cable length on node position is expressed as

$$\{dX\} = [L]\{dl\}, \qquad [L] = [M]^{-1} \tag{8}$$

If the number of cables whose lengths can be changed is restricted, deviation due to the length change of controllable cables is expressed as

$$\{dX\} = [Lc]\{dlc\} \tag{9}$$

where $\{dlc\}$ denotes the variation in lengths of cables whose lengths can be changed, and $[Lc]$ denotes the matrix generated by eliminating the columns of the matrix $[L]$ corresponding to the variations in uncontrollable cables. The surface error vector $\{e_i\}$, which is the deviation vector between the design and the measured position of ith node, is shown in Fig. 9. Total error vector $\{e_0\}$ is defined as

$$\{e_0\} = \{e_1 \ldots e_m\}^T \tag{10}$$

The following performance index is introduced to determine the control lengths of cables to correct the total error vector $\{e_0\}$:

$$I = \{e_0 + dX\}^T\{e_0 + dX\} \tag{11}$$

This index takes the following variational form:

$$\delta I = 2\delta\{dX^*\}^T\{e_0 + dX\} = 0 \tag{12}$$

where $\{dx^*\}$ is the resultant displacement vector due to the optimal control length vector $\{dl^*\}$.

The $\{dl^*\}$ is given as

$$\delta l = 2\delta\{dX^*\}^T\{e_0 + dX^*\} = 2\delta\{dlc\}^T[LC]^T\{e_0 + dX^*\} \tag{13a}$$

$$\{dl^*\} = ([Lc]^T[Lc])^{-1}[Lc]^T\{e_0\} \tag{13b}$$

Alternatively, if all of the cables' lengths can be adjusted, the optimal control vector $\{dl^*\}$ is given as

$$\{dl^*\} = [M]\{dX\} = -[M]\{e_0\} \tag{14}$$

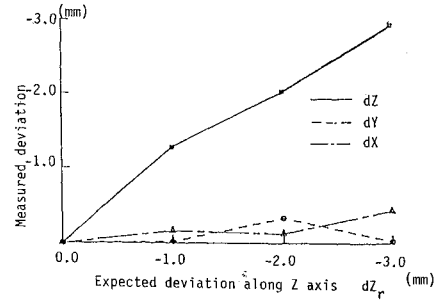

Fig. 15 Estimated and measured deviation of node 3.

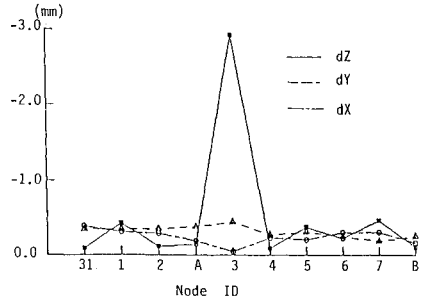

Fig. 16 Node deviations after $dZr = -3$ mm control.

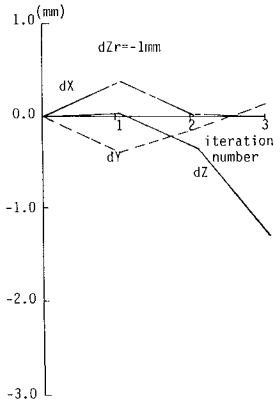

Fig. 17a Shape control sequence (d$Zr = -1$ mm).

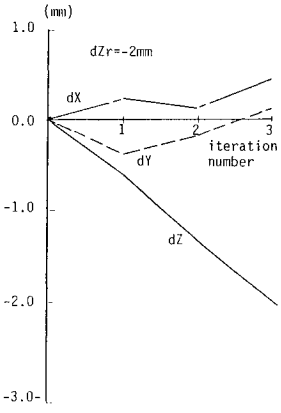

Fig. 17b Shape control sequence (d$Zr = -2$ mm).

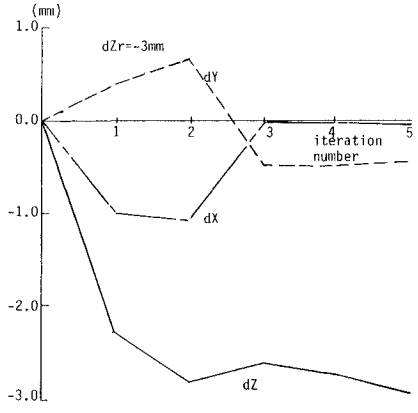

Fig. 17c Shape control sequence (d$Zr = -3$ mm).

The flowchart of the surface shape control algorithm is shown in Fig. 10.

Numerical Verification

The propriety of the previously mentioned shape control algorithm was verified by simulations using CASA. The simulation was performed in the following sequence:

1) Definition of distorted surface;
2) Surface rms error calculation;
3) Determination of the control cable lengths by using the control algorithm;
4) Addition of control cable lengths to the initial cable lengths; and
5) CASA calculation of the resultant node positions using modified cable lengths

Simulations were carried out on the same model used in the sensitivity analysis (Fig. 4), and two cable rigidities expressed in terms of the initial strain were considered. Smaller initial strain means a TTA, and larger initial strain means an antenna composed of flexible cable network. Figure 11 shows the results of the simulations. In this figure, σ/D denotes the surface rms error nondimensionalized by antenna aperture. The results of two simulations on each initial strain are shown in the figure. Deformation of a tension truss could be corrected after a few iterations of shape control. On the other hand, the convergence of the deformation of flexible network was slower than that of the rigid-cable network, because the rigid-cable assumption in the shape control algorithm was not appropriate in the cable networks whose cables have a 10^{-2} order strain. The shape control sequence is shown in Fig. 12. In the figure, broken lines indicate the design parabola, and the deviations are depicted at 300 times magnification.

Experimental Verification

Experiments were carried out to verify the shape control algorithm, but overall surface control verification could not be carried out due to the limitations of the view field of the position measurement apparatus, theodolites. The experiments only verified the controllability of a node on the surface. If the node could be translated without affecting the other node positions, it would assure the linear approximation of the control algorithm and the local controllability of the surface.

Theodolites were used to measure the node positions as shown in Fig. 13. Figure 14 indicates the node and cable identification and coordinate system, in which the Z direction corresponds to the parabola axis. The controlled node is number 3 in Fig. 14. Node 3 was controlled to translate along the parabola axis by d$Zr = -1$, -2, and -3 mm, where the subscript r denotes the value to be controlled. The rigidity of cables (EA) was 2500 kgf, and the estimated average tension of the cables was 1 kgf. Therefore, the initial strain of this model is on the order of 10^{-4}. Cable lengths were adjusted by turnbuckles at the midcord, and the adjustment limit of a turnbuckle was 0.02 mm. In the sequence of adjustment, it seemed that unexpected cable twisting caused shortenings of cables, and these shortenings were comparable to the adjustment amount, though an untwisting device was installed at each turnbuckle.

Table 1 shows the control cable lengths, which were obtained by linear analysis to shift node 3 by d$Zr = -1$, -2, and -3 mm. Values enclosed by parentheses in Table 1 are the exact solutions (according to rigid-cable mechanics) to obtain each dZr. It is shown that the linear control algorithm gives good approximations. Figure 15 shows the resultant position of node 3 after d$Zr = -1$, -2, and -3 mm control. In the figure, X- and Y-direction deviations are depicted with negative absolute value. Node 3 translates along the Z axis and hardly deviates along the X and Y axes. This verifies the local controllability of a node. Figure 16 shows the deviations of adjacent nodes after d$Zr = -3$ mm control. Node 3 translates without affecting the neighboring node positions. Deviations of fixed nodes, nodes A and B, might have been caused by the position measurement error and slight movement of the whole model during cable length controlling. These results were obtained through three-time (d$Zr = -1$ and -2 mm) or five-time (d$Zr = -3$ mm) iterations. The node 3 deviation sequence corresponding to adjustment iterations is shown in Fig. 17. The convergence of the iterations is not straightforward to the estimated value, and the error residuals might be large compared with the required deviation. These problems are most likely caused by the adjustment limit of turnbuckles and the shortening due to twisting. If more accurate shape control is required, more accurate length adjustment devices would be necessary.

Conclusion

This paper discussed the surface sensitivity to applied force errors and the shape control of a tension truss antenna (TTA). A concept model verified the feasibility of the TTA. Applied force error caused larger surface deformation in an antenna with a flexible cable network than in a TTA. It was also found that deformation of the surface can be controlled by changing the lengths of cables composing the surface, and the surface can be controlled locally. The shape control algorithm presented in this paper is considered applicable to the postfabrication adjustment, but in the future, in-orbit shape control will be included as a research target.

Acknowledgments

The authors wish to express their gratitude to Dr. Sergio Pellegrino of the University of Cambridge, Department of Engineering, for precious discussions and helpful advice, and also to Drs. Hiroaki Fuketa and Heiichi Yamamoto of NTT Radio Communication Systems Laboratories for their continuous support for this research.

References

[1]Archer, J. S., "Post-Fabrication Contour Adjustment for Precision Parabolic Reflectors," AIAA Paper 79-0933, May 1979.

[2]Belvin, W. K., Edighoffer, H. H., and Herstrom, C. L., "Quasi-Static Shape Adjustment of a 15 Meter Diameter Space Antenna," *Proceedings of the AIAA/ASME/ASCE/AHS 28th Structures, Structural Dynamics and Materials Conference,* AIAA, New York, April 1987, pp. 705–713.

[3]Kitamura, T., Okazaki, K., Natori, M., Miura, K., Sato, S., and Obata, A., "Development of a 'Hingeless Mast' and its Applications," *Acta Astronautica,* Vol. 17, No. 3, March 1988, pp. 341–346.